Macromolecules

pubs.acs.org/Macromolecules Article

Closed-Loop Recyclable Aliphatic Poly(ester-amide)s with Tunable Mechanical Properties

Yu-Ting Guo, Changxia Shi, Tian-Yi Du, Xiang-Yue Cheng, Fu-Sheng Du,* and Zi-Chen Li*

Cite This: *Macromolecules* 2022, 55, 4000−4010 Read Online

ACCESS | Metrics & More | Article Recommendations | Supporting Information

ABSTRACT: The design and synthesis of closed-loop recyclable polymers is a promising solution to address the large negative effects of plastic pollution problem and massive economic loss associated with single-use plastics. We demonstrate that ring-opening polymerization (ROP) of 6-alkyl-substituted morpholine-2,5-dione (MDs) leads to closed-loop recyclable aliphatic poly(ester-amide)s (PEAs) with tunable mechanical properties. The controlled ROP of these MDs was achieved using benzyl alcohol as an initiator and DBU/TU as a catalyst, affording various PEA homo- and copolymers with different molar masses and compositions. All these PEAs are amorphous and thermally stable with $T_{d,5\%}$ values in the range of 267−292 °C. Their glass transition temperatures (T_g) are in the range of 58−142 °C, being affected by the structure of pendent alkyl groups, the hydrogen bonding between amide groups, and the composition of copolymers. Tensile tests revealed that the structure of pendent alkyl groups exerts a significant effect on the mechanical property of PEAs, and they are brittle (*n*-butyl or cyclohexyl substituted) or ductile (*n*-hexyl or *n*-octyl substituted) plastics. In addition, the mechanical properties of PEAs could be finely adjusted by the copolymerization of different MD monomers. Of importance, both homopolymers and copolymers of these PEAs could be thermally depolymerized by sublimation to recover the corresponding monomers in high purity and efficiency. Given their good and adjustable thermal/mechanical properties, and excellent recyclability, these PEAs show promise as new close-loop recyclable polymers.

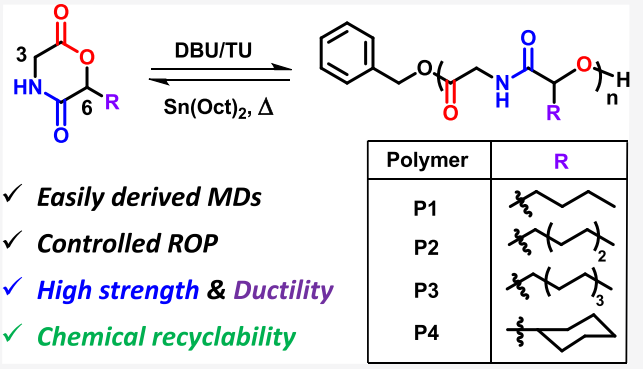

INTRODUCTION

Synthetic polymers, known for their excellent durability, processability, low density, and other diverse properties, have become indispensable in our daily life. However, the increasing production and extensive single-use of nondegradable synthetic plastics brings concerns of resource waste and environmental pollution owing to their high stability.[1−3] Efforts to address these issues include the development of new biodegradable polymers and finding feasible means to (up)recycle commercial plastics. It has been found that most biodegradable polymers can be efficiently degraded in laboratory experiments but show a drastically different degradation kinetics under normal environmental conditions.[4,5] At present, mechanical and chemical recycling are the two most widely used methods to deal with waste plastics, whereas they either cause significant quality loss or need a large amount of organic solvents.[6−8] An attractive alternative strategy is to design new chemically recyclable polymers that can depolymerize back into their constituent monomers and subsequently repolymerize them to the virgin-quality materials.[9−11] Although the process of depolymerization can be energetically costly and catalysts should be used, this closed-loop recycling is a potentially sustainable solution to recycling waste plastics.

Polymers generated via ring-opening polymerization (ROP) of low-strained cyclic monomers are supposed to be intrinsically depolymerized back into their corresponding cyclic monomers above their ceiling temperatures. Polyesters from the ROP of cyclic ester monomers are among the most extensively investigated chemically recyclable polymers. This has been demonstrated with monomers ranging from five- to seven-membered lactones, each of them needs a tailored structure to reach an appropriate balance between polymerization and depolymerization.[12−18] These monomers can undergo ROPs at high monomer concentrations and low temperatures to afford polyesters with high monomer conversions. These polyesters are kinetically thermally stable in the bulk states for real applications, while in the presence of suitable catalysts, they can be selectively depolymerized into

Received: January 28, 2022
Revised: April 20, 2022
Published: May 10, 2022

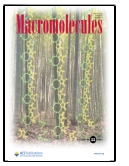

https://doi.org/10.1021/acs.macromol.2c00221
Macromolecules 2022, 55, 4000−4010

the original monomers at elevated temperatures or in diluted solutions.[9,10,15,16]

Poly(ester-amide)s (PEAs) contain both ester and amide motifs in their backbones, which combine the excellent thermal/mechanical properties of polyamides and the degradability of aliphatic or some semi-aromatic polyesters. PEAs can be synthesized via polycondensation of difunctional monomers or ROP of cyclic monomers.[19,20] The ROP of the cyclic monomers containing both ester and amide in the ring is not only atom-economical but can also afford PEAs with a perfectly alternating ester-amide sequence distribution. In addition, the obtained PEAs may possess the potential to be chemically depolymerized if the ester and amide motifs are carefully arranged along the polymer backbones. Hocker and coworkers synthesized a series of 11- to 14-membered cyclic ester-amide monomers, ROPs of which were carried out at high temperatures, being accompanied by obvious side reactions like transesterification.[21,22] These PEAs were not suitable for chemical recycling to recover the corresponding monomers. The six-membered morpholine-2,5-dione derivatives (MDs) are an important class of cyclic ester-amide monomers and have been extensively studied.[23] Most of the MDs contain different side groups at the 3-position, being prepared from the versatile amino acid feedstocks via traditional synthetic routes. In general, these methods have drawbacks such as low overall yields and difficulty of introducing substituents at the 6-position of MDs.[24] Moreover, the ROPs of MDs were mostly carried out with enzymes or metal compounds, yielding PEAs with relatively low molar mass and broad dispersity.[25,26]

We have recently reported a simple method for the efficient synthesis of MDs based on the Passerini-type reaction. By using different aldehydes and isocyanides derived from α-amino acids, various MDs with substituents at 3- and/or 6-positions can be easily prepared, which greatly expands the structural diversity of MDs. We also demonstrated that the diazabicyclo[5.4.0]undec-7-ene (DBU)/1-(3,5-Bis-(trifluoromethyl)-phenyl-3-cyclohexyl-2-thiourea) (TU)-catalyzed ROP of MDs was well controlled. Some of the obtained PEAs could be depolymerized back into the corresponding monomers catalyzed with acids, indicating that PEAs generated by the ROP of MDs represent a new type of promising polymers with chemical recyclability.[27] Nevertheless, these reported PEAs were brittle, and more efforts are necessary to improve their material performance. To translate the recyclable polymers into useful materials in real applications, the tradeoffs between the recyclability and mechanical performance need to be well addressed.[11,28,29] It is well known that side groups can greatly influence the thermal and mechanical properties of polymers.[30−32] We hypothesize that the introduction of the *n*-alkyl group at the 6-position of MDs could enhance the ductility of the PEAs while maintaining their mechanical strength as a consequence of hydrogen bonding interactions. Notably, these 6-substitued MDs with various side groups can be easily tailored from different aldehydes, which allows the facile tuning of PEA material properties. Furthermore, these PEAs could be thermally depolymerized via sublimation to recover the corresponding MD monomers with a high efficiency (Scheme 1).

Scheme 1. ROPs of MDs and Chemical Recycling of PEAs via Depolymerization

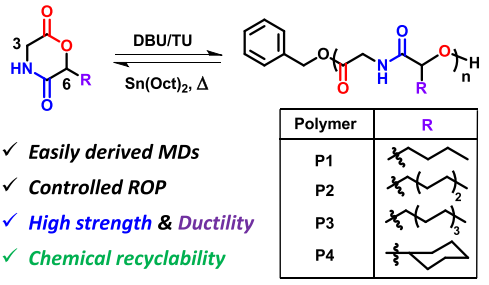

EXPERIMENTAL PART

Materials. Ethyl isocyanoacetate (Meryer, 98%), boric acid (Xilong, 99%), valeraldehyde (Macklin, 98%), heptaldehyde (Macklin, 98%), nonaldehyde (J&K, 95%), cyclohexanaldehyde (Bide, 95%), 4-methylbenzenesulfonic acid (*p*-TsOH, 99%, Xiya Reagent), diazabicyclo[5.4.0] undec-7-ene (DBU, J&K, 98%), and benzyl alcohol (J&K , H_2O < 30 ppm) were purchased from commercial suppliers and used directly. 1-(3,5-Bis(trifluoromethyl)-phenyl-3-cyclohexyl-2-thiourea) (TU) was synthesized according to the published procedure.[33]

Measurements. ^{1}H and ^{13}C NMR spectra were recorded on a Bruker Avance 400 or 500 MHz spectrometer using tetramethylsilane as the reference. Fourier transform infrared (FT-IR) spectroscopy was performed on a Thermoscientific (Nicolet iS50) FT-IR spectrometer equipped with a temperature controller. For the temperature-dependent FT-IR measurements, the sample was heated from 30 to 100 °C, and the spectra were recorded every 10 °C in the wavenumber range of 800−4000 cm^{-1}. Electrospray ionization (ESI) mass spectra were recorded on a Bruker Solarix XR Fourier transform mass spectrometer in the positive ion mode with a high resolution. Matrix-assisted laser desorption ionization time-of-flight mass spectroscopy (MALDI-TOF MS) was performed on the AB Sciex 5800 mass spectrometer. α-Cyano-4-hydroxycinnamic acid was used as the matrix, and the spectrum was acquired in cation reflection mode. Size exclusion chromatography (SEC) measurements were performed on a Waters system equipped with a Waters 1525 binary HPLC pump, a Waters 2414 refractive index detector, and three Waters Styragel HT columns (HT2, HT3, HT4) thermostated at 35 °C. Tetrahydrofuran (THF) was used as the eluent at a flow rate of 1.0 mL/min. The calibration was made against a series of polystyrene standards with narrow distribution. The data were collected and processed with a Breeze software. Thermogravimetric analysis (TGA) was performed on a Q600-SDT thermogravimetric analyzer (TA Co. Ltd.). Polymer samples were heated from 50 to 600 °C at a heating rate of 10 °C/min under a nitrogen flow of 100 mL/min. Decomposition onset temperatures (T_d) of the polymers were defined at 5% weight loss. Differential scanning calorimetry (DSC) was performed on a TA Q100 differential scanning calorimeter. Polymer samples were heated from −40 to 200 °C at a heating/cooling rate of 10 °C/min under a nitrogen flow of 50 mL/min. Data of the endothermic thermograms were recorded from the second scan after the removal of thermal history and analyzed with a TA Universal Analysis software.

The bulk static tensile properties of polymer samples were measured using an Instron 5567 instrument with a 5 kN load cell. Dumb-bell-shaped samples (GB/T 4B specimens, 12 mm × 2 mm × 1 mm) were made by hot-pressing in a stainless-steel mold under 10 MPa pressure at 20 °C above the T_g of the sample for 30 min and stretched at a strain rate of 1 mm/min at ambient temperature until break. The measurements were performed in triplicate, and the average values with standard errors were calculated.

Synthesis of MDs. Detailed synthetic procedures and characterizations of monomers, **M1**, **M2**, **M3**, and **M4**, are provided in the Supporting Information.

ROP of M1−M4. The ROP of **M1** catalyzed by DBU/TU was described as a representative procedure (Table 1, entry 2). In a N_2-filled glovebox, **M1** (2.56 g, 15 mmol, 200 equiv) and TU (138.9 mg, 0.375 mmol, 5 equiv) were dissolved in DCM (19.8 mL) in a 50 mL

https://doi.org/10.1021/acs.macromol.2c00221
Macromolecules 2022, 55, 4000−4010

Table 1. Synthesis and Characterization of P1−P4[a]

entry	polymer	$[M]_0/[I]_0$	time (h)	conv. (%)[b]	$M_{n,theo}$ (kDa)[c]	M_n (kDa)[d]	$Đ$[d]	T_d (°C)[e]	T_g (°C)[f]
1	**P1a**	20	1	98	3.4	3.3	1.11	–	–
2	**P1b**	200	8	96	32.2	19.2	1.21	272	78.7
3	**P1c**	400	21	95	65.1	28.2	1.36	278	80.5
4	**P2a**	20	1	94	3.9	4.4	1.07	–	–
5	**P2b**	200	8	90	35.9	25.6	1.14	269	60.2
6	**P2c**	400	21	89	70.9	35.1	1.22	280	65.0
7	**P3a**	20	1	96	4.5	4.8	1.06	–	–
8	**P3b**	200	8	89	40.5	27.0	1.08	290	58.9
9	**P3c**	400	21	87	77.7	44.0	1.27	290	60.4
10	**P4a**	20	1	96	3.9	3.3	1.09	–	–
11	**P4b**	400	120	88	69.5	13.8	1.31	267	141.8

[a]All Polymerizations were conducted in DCM at 30 °C in a glovebox under N_2 using BnOH as the initiator and DBU/TU as the catalyst. $[BnOH]_0/[DBU]/[TU] = 1/1/5$, $[M]_0 = 0.6$ M in DCM. **P1−P4** were obtained by ROP of the corresponding monomers **M1−M4**. [b]Determined by ^{1}H NMR. [c]Calculated from Conv. × ($[M]_0/[I]_0$) × (MW of **M**) + MW of BnOH). [d]Determined by SEC using THF as the eluent and PS standards. [e]Determined by TGA. [f]Determined by DSC.

vial containing a microstirring bar, then 100 μL of BnOH solution (0.75 M in DCM) and 100 μL of DBU solution (0.75 M in DCM) were sequentially added to the vial. The mixture was stirred at 30 °C. After 8 h, the polymerization was quenched by adding excess benzoic acid solution. The crude product was purified by three successive precipitations from diethyl ether and dried in vacuo. Pure **P1b** was obtained as a transparent solid (2.0 g, 78%). ^{1}H NMR (400 MHz, $CDCl_3$) δ: 8.38−7.74 (m, 1H), 5.18 (m, 1H), 4.38−3.68 (m, 2H), 2.14−1.59 (m, 2H), 1.50−1.20 (m, 4H), 1.05−0.69 (m, 3H). ^{13}C NMR (126 MHz, $CDCl_3$) δ172.43, 168.27, 74.69, 42.04, 31.40, 26.89, 22.24, 13.82.

The experimental procedure was the same as that for the ROP of **M2−M4**. Because of the difference in solubility of these polymers, different solvents were applied for precipitation: diethyl ether for **P1a−P1c** and **P4a−P4c**, diethyl ether/petroleum ether (1/1, v/v) for **P2a−P2c**, and acetonitrile for **P3a−P3c**. The overall yields of these PEA homopolymers are **P1a** (152 mg, 86%), **P1c** (1.8 g, 70%), **P2a** (181 mg, 88%), **P2b** (1.9 g, 63%), **P2c** (2.2 g, 73%), **P3a** (134 mg, 58%), **P3b** (2.4 g, 70%), **P3c** (2.2 g, 64%), **P4a** (134 mg, 58%), and **P4b** (2.4 g, 70%).

Copolymerization of M3 and M4. A representative example (Table 3, entry 5) is given. In a N_2-filled glovebox, **M3** (1.36 g, 6.0 mmol, 200 equiv), **M4** (1.18 g, 6.0 mmol, 200 equiv), and TU (55.5 mg, 0.15 mmol, 5 equiv) were dissolved in DCM (20.8 mL) in a 50 mL vial containing a microstir bar, then 100 μL of BnOH solution (0.3 M in DCM, 1 equiv) and 100 μL of DBU solution (0.3 M in DCM, 1 equiv) were added to the vial sequentially. The mixture was stirred at 30 °C. The polymerization process was monitored by ^{1}H NMR. After the reaction was completed, excess benzoic acid solution was added to quench the reaction. The copolymer was purified by three successive precipitations from cold acetonitrile and dried in vacuo to provide **C5** as a transparent solid (1.8 g), and the overall yield is 71%. The molar fraction of two monomer units was calculated by ^{1}H NMR. Copolymers with different compositions were prepared by changing the feed ratio of two monomers under the same condition.

Kinetic Studies. The homopolymerization of **M1** catalyzed by DBU/TU was described as a representative procedure for the studies of kinetics. In a N_2-filled glovebox, **M1** (352.2 mg, 2.0 mmol, 100 equiv) and TU (37.0 mg, 0.1 mmol, 5 equiv) were dissolved in DCM (4.3 mL) in a 20 mL vial containing a microstir bar, then 100 μL of BnOH solution (0.2 M in DCM, 1 equiv) and 100 μL of DBU solution (0.2 M in DCM, 1 equiv) were added to the vial sequentially. The mixture was stirred at 30 °C. At a specific time, 40 μL of the reaction solution was taken out and transferred into a nuclear magnetic resonance (NMR) tube, and quickly quenched by adding 50 μL of benzoic acid solution (1 M in DCM). After removing the solvent in vacuo, the residue was redissolved in $CDCl_3$ for ^{1}H NMR measurement or in THF for SEC characterization. For the other monomers (**M2−M4**) or the copolymerization kinetics of **M3** and **M4**, the experimental procedure was the same as mentioned above.

Depolymerization of (Co)Polymers to Recover Monomers. Thermal depolymerization of polymers and recovery of monomers were carried out by sublimation in vacuo using the polymer samples after uniaxial tensile tests. Take **P3b** as an example. 200 mg of PEO and 5 mg of $Sn(Oct)_2$ were added into a sublimation device with a microstirring bar and heated at 140 °C for 2 h in vacuo. After cooling to ambient temperature, the cold finger was cleaned up, and 202 mg of **P3b** was added. The mixture was further stirred at 140 °C in vacuo for a certain time, and the sublimate was collected. The amount of sublimate was used to calculate the yield, and the purity of the sublimate was characterized by ^{1}H NMR. The depolymerization procedure was the same for other homo- and copolymers.

RESULTS AND DISCUSSION

Synthesis of 6-Substituted MDs. To obtain PEAs with tunable mechanical properties and recyclability, we have designed four 6-substituted MD monomers (**M1−M4**) containing pendent *n*-butyl, *n*-hexyl, *n*-octyl, and cyclohexyl groups, respectively. They were synthesized by two steps of reactions (Scheme 2). The intermediate compounds **1−4** were

Scheme 2. Synthesis and Chemical Structure of M1−M4

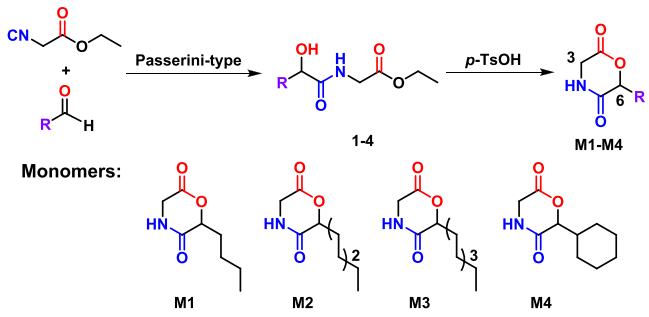

prepared from commercially available ethyl isocyanoacetate and different aldehydes via the boric acid-catalyzed Passerini-type reaction in yields of 61−93%.[34] Then, **M1−M4** were simply obtained by the acid-catalyzed intramolecular cyclization of **1−4** with overall yields of 38−72%. The detailed synthetic procedure and characterization data are given in the Supporting Information (Figures S1−S5).

Synthesis of PEA Homopolymers. The ROP of MDs has been investigated recently with the catalysis of 1,8-

https://doi.org/10.1021/acs.macromol.2c00221
Macromolecules 2022, 55, 4000−4010

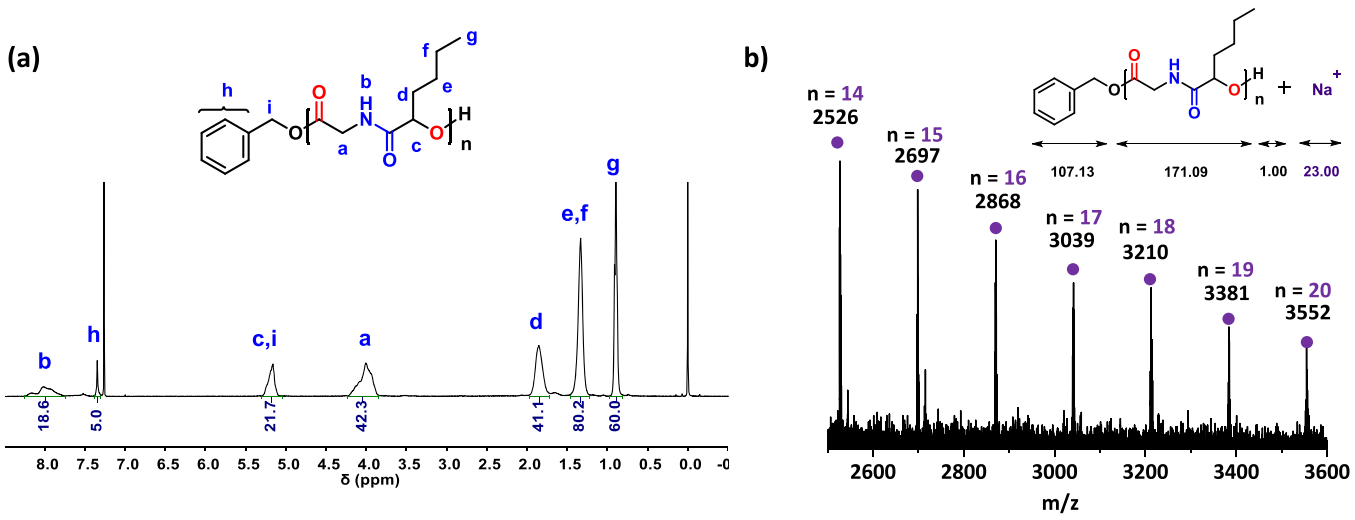

Figure 1. (a) ^{1}H NMR and (b) MALDI-TOF MS spectra of **P1a** (Table 1, entry 1).

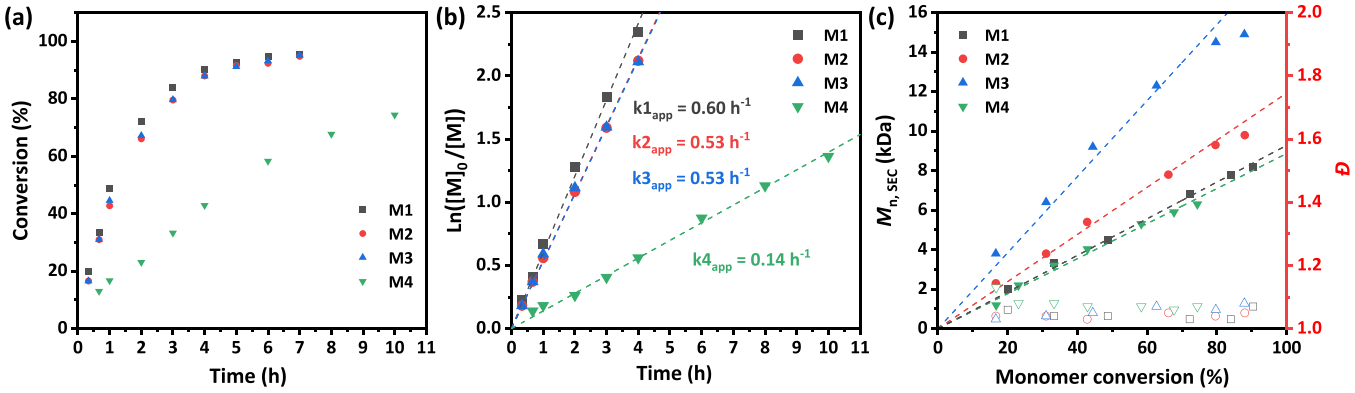

Figure 2. Kinetics study of the homopolymerization of **M1**−**M4**: (a) monomer conversion vs time; (b) semilogarithmic kinetic plots; (c) plots of polymer molar mass (M_n) and dispersity ($Đ$) vs monomer conversion.

diazabicyclo[5.4.0]undec-7-ene (DBU) or triazabicyclo[4.4.0]-dec-5-ene (TBD).[27,35] The polymerizations were not well controlled using DBU or TBD alone as the catalyst, probably due to the deprotonation of amide in MDs. The in situ-generated amide anions could also initiate the ROP of MDs but with a poor controllability.[35] To prevent this undesired deprotonation of amide, thiourea (TU) was used as the cocatalyst, affording a significantly improved controllability of the ROP. The DBU/TU or TBD/TU binary catalyst system has been successfully applied to the controlled ROP of MDs with different substituents.[27,36,37] Herein, we employed the DBU/TU catalyst system to synthesize **P1**−**P4** from the corresponding monomers **M1**−**M4**, using benzyl alcohol (BnOH) as the initiator and with the BnOH/DBU/TU ratio fixed at 1/1/5. At a low monomer to initiator ratio (20/1), the ROP of **M1**−**M4** achieved high conversions within 1 h (Table 1, entries 1, 4, 7, and 10), the molar masses of the obtained **P1a**−**P4a** were close to the theoretical values, and all of them exhibited low dispersities ($Đ$ < 1.2). These polymers were characterized by ^{1}H/^{13}C NMR and MALDI-TOF MS spectra. The representative ^{1}H NMR and MS spectra of **P1a** are shown in Figure 1, which clearly indicated that the ROP of **M1** was initiated by BnOH. The chemical structures of **P2a**−**P4a** were also confirmed by NMR and MS spectra (Figures S6−S9).

By increasing the initial ratio of the monomer to the initiator, we could obtain polymers of a high molar mass. However, a much longer reaction time was necessary to reach high monomer conversion, in particular, for the ROP of **M4** (Table 1, entry 11). Accordingly, the dispersities of the polymers became slightly broader because of the trans-esterification between polymer chains. Moreover, at the high ratios of monomer to initiator, the molar masses measured by SEC were much lower than theoretical values that were calculated according to monomer conversion, which is probably due to that some polymer chains were initiated by trace water instead of BnOH.

To explore the effect of the substituent at 6-position on the polymerization of MDs, we further studied the ROP kinetics of **M1** to **M4** under the same condition ($[M]_0$/$[BnOH]_0$/[DBU]/[TU] = 100/1/1/5, 30 °C in DCM) by using ^{1}H NMR and SEC. As shown in Figure 2b, all the monomers followed a first-order kinetics, and their apparent ROP rate constants (k_{app}) were 0.60 h^{-1} (**M1**), 0.53 h^{-1}(**M2**), 0.53 h^{-1}(**M3**), and 0.14 h^{-1} (**M4**), respectively. In comparison with the *n*-alkyl-substituted monomers (**M1**−**M3**), the drastically slower rate of **M4** is most likely due to the more steric hindrance of the cyclohexyl group on the ROP of **M4**. A similar phenomenon was observed in the ROP of *rac*-dicyclohexylglycolide, whose polymerization rate is 1/70 of that of *rac*-lactide.[38] Moreover, monomers **M1**−**M3** showed similar rate constants, which are close to that of 6-(9-decenyl)-morpholine-2,5-dione,[27] indicating that the length of the *n*-

https://doi.org/10.1021/acs.macromol.2c00221
Macromolecules 2022, 55, 4000−4010

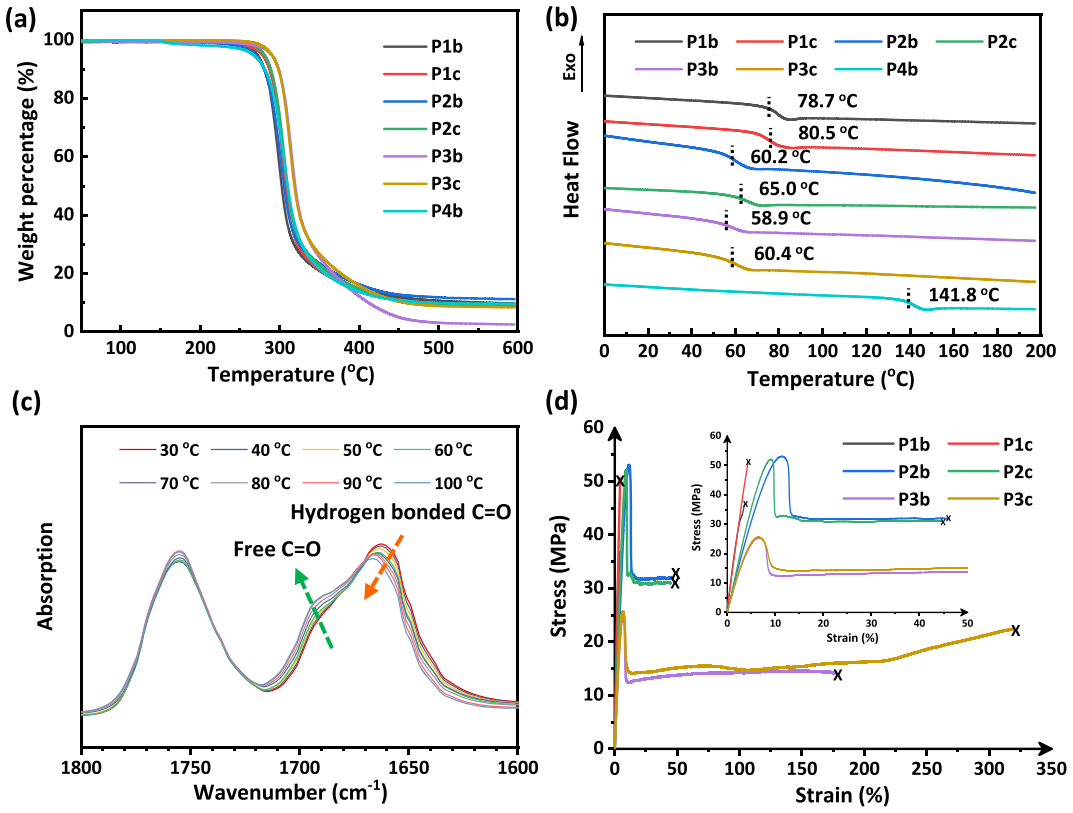

Figure 3. (a) TGA and (b) DSC thermograms of **P1**−**P4**; (c) variable temperature FT-IR of **P3c** in the 1600−1800 cm^{-1} region; (d) Stress−strain curves of **P1**−**P3** and the regional enlarged view.

alkyl chain at the 6-position exhibited a negligible effect on the ROP of MDs. Recently, Giani and coworkers studied the ROP kinetics of 3S-(isobutyl)-morpholine-2,5-dione under the similar condition ($[M]_0/[BnOH]_0/[DBU]/[TU]$ = 100/1/1/5, 40 °C in DCM) and obtained a k_{app} of ∼24 h^{-1}, which is ∼40−45 folds of that of **M1**−**M3**.[37] The significantly slower ROP rates of the 6-alkyl-substituted MDs compared with the 3-alkyl-substituted counterpart could be attributed to the less-active propagating chain end (secondary alkoxide) during the former's ROP.

Figure 2c shows that there was a linear relationship between the polymer molar masses and the monomer conversion (≤80%), and the dispersities were relatively low throughout polymerization, demonstrating the good controllability for the ROP of **M1**−**M4** catalyzed by DBU/TU. We also briefly examined the impact of the solvent and temperature on the ROP of **M3**. The ROP of **M3** was carried out in THF at 30 and 60 °C, respectively, while maintaining the other conditions same as in DCM. The obtained k_{app} value for **M3** in THF is only 0.06 h^{-1} at 30 °C, greatly lower than that in DCM. Increasing the temperature from 30 to 60 °C, the k_{app} of **M3** was increased only moderately (∼1.3 fold), but the dispersities of the polymers became broader most probably due to the inter- and intramolecular transesterification side reaction (Figure S10).

Thermal and Mechanical Properties of PEA Homopolymers. The thermal stability of the above polymers with relatively high molar masses was evaluated by TGA (Figure 3a), their 5% weight loss temperatures ($T_{d,5\%}$) were in the range of 267−290 °C. Among these tested polymers, **P3b** and **P3c** with the longest alkyl side chain showed the highest $T_{d,5\%}$ (290 °C), which is similar to that of crystalline poly(L-lactide) PLLA.[39] DSC results revealed that all these polymers are amorphous, owing to the irregular stereochemistry of side chains.[40] Their glass transition temperatures (T_g) are in the range of 59−142 °C (Figure 3b). With the same structure, the polymers with higher molar mass (**P1c**−**P3c**) exhibited a slightly higher T_g than their low molar mass analogues (**P1b**−**P3b**). Moreover, T_g was decreased sequentially from 80.5 °C for **P1c** to 65.0 °C for **P2c**, and to 60.4 °C for **P3c**, being moderately influenced by the length of the side chain (Table 1). A similar phenomenon was observed in other polymer systems such as poly(*n*-alkyl methacrylates) and *n*-alkyl-substituted polyalkylglycolides. For these two types of polymers, the introduction of long *n*-alkyl substituents remarkably reduced their T_gs to well below room temperature, for instance, T_g decreased from 20 °C for poly(*n*-butyl methacrylates) to −20 °C for poly(*n*-octyl methacrylates).[31,41] In contrast, all three kinds of PEAs (**P1**−**P3**) with M_n ∼ 19−44 kDa have much higher T_gs and are plastic materials at room temperature, which is attributed to the hydrogen bonding interactions between the amide groups in PEA main chains. For **P4b**, the less-flexible cyclohexyl group was directly attached to the PEA backbone, possessing a T_g of 141 °C. The greatly increased T_g can be explained by the combined effects of sterically hindered substituents and hydrogen bonding interactions.[31] The introduction of cyclohexyl to polymers will increase the rotational barriers along the polymer backbone and lead to a higher T_g.[38,42] Likewise, the intra- and intermolecular hydrogen bonding in the polymer retards the mobility of polymer chains, which would also result in an increased T_g.[43] The FT-IR measurements were conducted to prove the hydrogen bonding interaction between amide groups. As shown in Figure 3c, with increasing temperature

https://doi.org/10.1021/acs.macromol.2c00221
Macromolecules 2022, 55, 4000−4010

from 30 to 100 °C, the carbonyl absorption of the H-bonded amide at ∼1660 cm^{-1} gradually decreased, whereas the signal of free amide (∼1690 cm^{-1}) increased, being associated with the partial dissociation of hydrogen bonds.[44,45]

Overall, **P1**−**P4** are amorphous materials and show good thermal stability, and all of them have a relatively wide processing temperature range. It is interesting to note that T_g of the isomer of **P2** that contains *n*-hexyl substituent at the 3-position was 30 °C lower than **P2**, which is probably attributed to the weakened hydrogen bonding between amides induced by the adjacent alkyl groups at the 3-position.[46]

Uniaxial tensile tests were carried out to examine the mechanical properties of **P1**−**P3** (b and c series). The dog-bone-shaped specimens were prepared by hot-pressing, and they are all transparent. The length of the pendent *n*-alkyl substituents has a dramatic impact on the mechanical properties (Figure 3d and Table 2). A general trend was observed for **P1**−**P3**, that is, Young's modulus (E), yield stress (σ_y), and tensile stress (σ_b) gradually decreased along with the increase in the side chain length, whereas the strain at break (ε_b) followed a reverse tendency. Polymer **P1** samples are brittle plastics with a small ε_b (4−5%) and the largest E (1.1−1.3 GPa). In contrast, both **P2** and **P3** are ductile materials. Polymer **P2c** exhibited the E of 743 MPa, σ_y of 52.3 MPa, σ_b of 31 MPa, and ε_b of 45%. With further prolonging the pendent *n*-alkyl length, the ε_b of **P3c** reached 330%, despite a moderate decrease in its E (563 MPa) and σ_b (24.8 MPa) as compared to **P2c**. Both **P2** and **P3**, **P3c** in particular, are superior in their ductility over some reported thermal recyclable polyesters such as PLLA and Poly(3,4-T6GBL),[12,39] while maintaining a moderate mechanical strength.

Table 2. Mechanical Properties of P1−P3[a]

polymer	E/MPa	σ_y/MPa	σ_b/MPa	ε_b/%
P1b	1276 ± 14	–	43.9 ± 10.3	4.0 ± 0.9
P1c	1134 ± 102	–	51.0 ± 1.4	4.8 ± 0.5
P2b	623 ± 33	49.9 ± 6.0	30.5 ± 3.0	45.7 ± 6.3
P2c	743 ± 22	52.3 ± 0.9	31.4 ± 0.5	45.1 ± 6.0
P3b	541 ± 16	25.9 ± 2.3	15.1 ± 1.7	216.6 ± 40
P3c	563 ± 15	27.4 ± 1.8	24.8 ± 2.4	332.6 ± 14

[a]Tested by uniaxial tensile tests. E: Young's modulus; σ_y: yield stress; σ_b: breaking stress; ε_b: strain at break.

Phase Structure of PEA Homopolymers. To understand the relationship between the polymer microphase structure and material properties, **P1c**−**P3c** were further characterized by wide-angle X-ray diffraction (WAXD). **P1c**−**P3c** showed a broad peak at q = 14.2 nm^{-1} and a relatively narrow peak at low angles but did not exhibit any sharp reflection peak (Figure 4a). This is consistent with the DSC results, indicating their amorphous structures. The low-angle reflection peak gradually shifted to a low q value upon increasing the side chain length, the corresponding d-spacing values (1.42 nm for **P1c**, 1.81 nm for **P2c**, 2.18 nm for **P3c**) showed a good linear relationship with the side chain carbon atom number (Figure 4b). On the basis of above WAXD results, we proposed a double-layer molecular packing mode for these PEAs (Figure 4c). The side chains are arranged on two sides of the twisted PEA main chains, and such a packing mode is driven by the incompatibility of nonpolar alkyl groups and the polar ester/amide moieties. From the linear fit, the increase in the double-layer spacing per carbon atom is 0.19 nm, which is approximately consistent with all-*trans* conformations of the alkyl side chains. The intercept of 0.66 nm represents the size of the twisted PEA main chain without counting the side alkyl

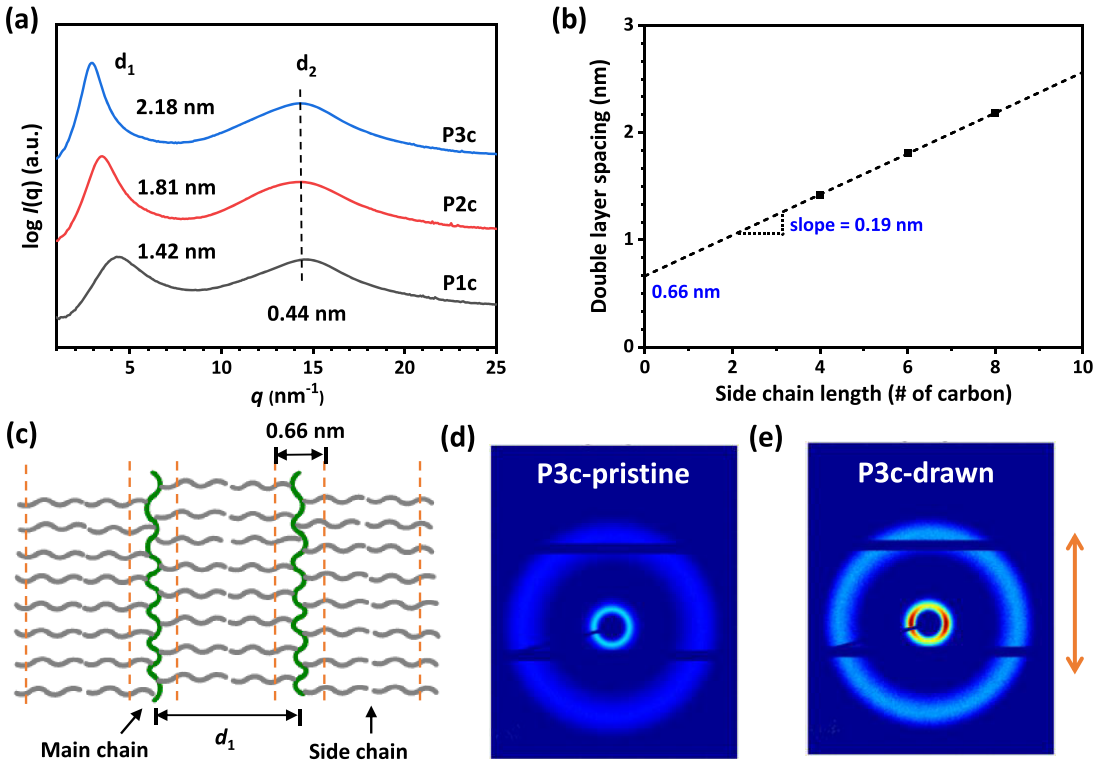

Figure 4. (a) 1D-WAXD profiles and (b) plot of d-spacing versus side chain length for **P1c**−**P3c**; (c) proposed double-layer molecular packing model. 2D-WAXD patterns of (d) pristine and (e) tensile-deformed **P3c**.

https://doi.org/10.1021/acs.macromol.2c00221
Macromolecules 2022, 55, 4000−4010

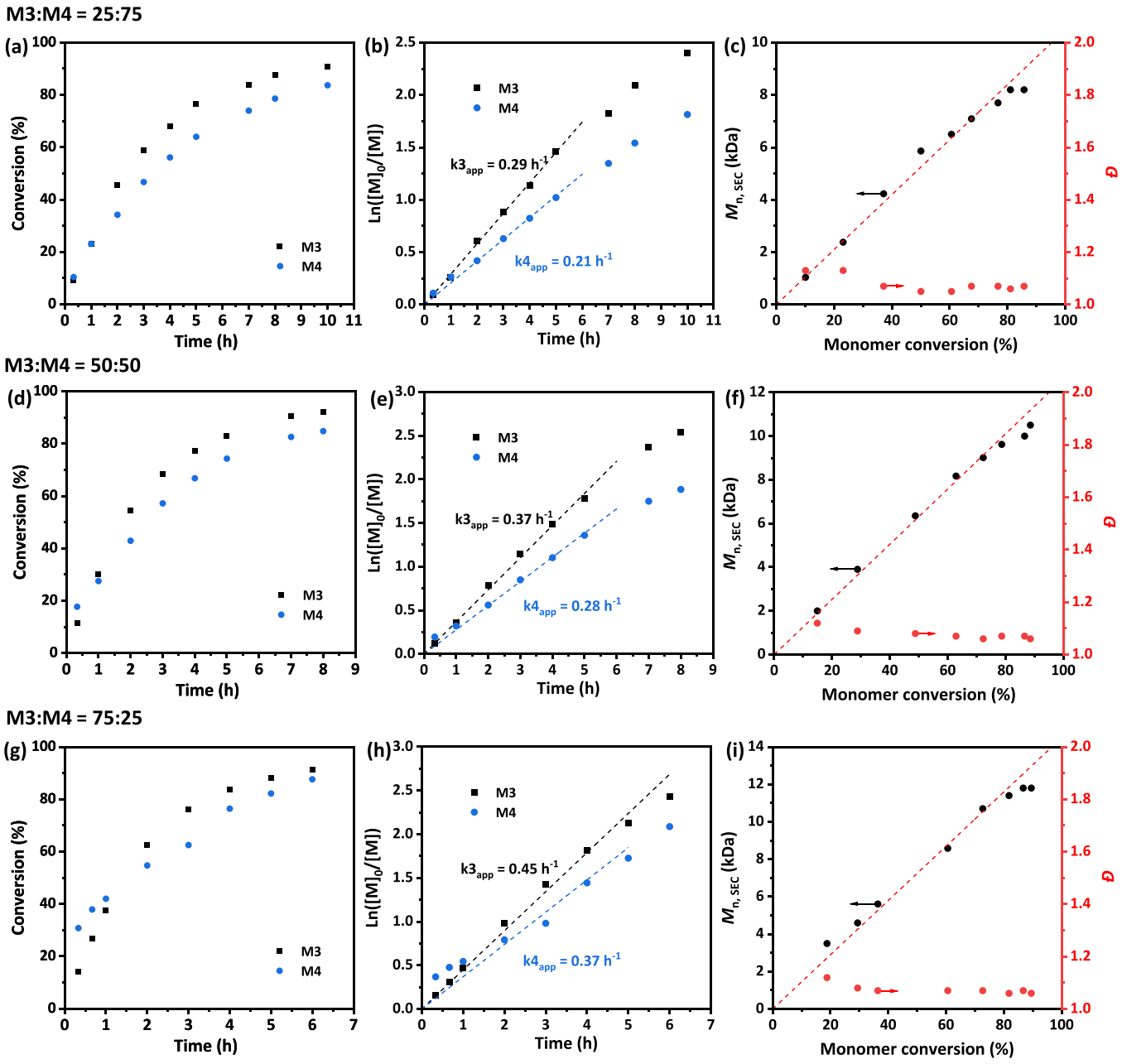

Figure 5. Kinetic study of the copolymerization of **M3** and **M4**: (a,d,g) monomer conversion vs time; (b,e,h) semilogarithmic kinetic plots; (c,f,i) plots of copolymer molar mass (M_n) and dispersity ($Đ$) vs monomer conversion.

chains.[47] The broad reflections q = 14.2 nm^{-1}, corresponding to a 0.44 nm d-spacing, did not shift with the length of side chains. This d-spacing (0.44 nm) could be correlated to the conventional van der Waals interaction and/or hydrogen bonding between the neighboring polymer main chains.[48]

Then, we employed 2D-WAXD to reveal the microstructure change in **P1**−**P3** induced by tensile deformation. The 2D-WAXD patterns of pristine **P1c**−**P3c** specimens were all isotropic (Figures 4d and S11a,b). After being stretched, the broken specimens of **P1c** and **P2c** retained the isotropic microstructure (Figure S11c,d); in contrast, an anisotropic 2D-WAXD pattern was clearly observed for **P3c** (Figure 4e). The scattering intensity of the low-angle reflection was greatly enhanced in the equatorial direction, indicating that the double-layer nanophases were oriented along the polymer chain orientation, that is, the stretching direction (Figure S12). This result is consistent with the up-curved stress−strain curve in the region of large strain for **P3c** (Figure 3d). It is well known that the orientation of polymer chains or ordered nanophases upon stretching can increase the tensile strength along the stretching direction.[49]

Synthesis and Properties of PEA Copolymers. Copolymerization is a practical manner to adjust the polymer properties.[50] **P4** with a cyclohexyl side chain shows the highest T_g among the four PEAs, but it is very brittle at room temperature. Considering the good ductility but a relatively low T_g of **P3c**, we speculate that the ring-opening copolymerization (ROCP) of **M3** and **M4** may afford copolymer materials with a broad scope of thermomechanical properties. First, we studied the copolymerization kinetics under the same condition as for homopolymerization (([**M3**]$_0$ + [**M4**]$_0$)/[BnOH]$_0$/[DBU]/[TU] = 100/1/1/5), only

https://doi.org/10.1021/acs.macromol.2c00221
Macromolecules 2022, 55, 4000−4010

changing the feeding ratios of **M3** to **M4** from 25:75 to 50:50, and to 75:25, ^{1}H NMR and SEC were also used to monitor the copolymerization process (Figure S13). High monomer conversions (80%) were observed for **M3** and **M4** within 10 h (Figure 5a,d,g), and both monomers followed pseudo-first-order kinetics (Figure 5b,e,h). In each of these experiments, **M3** showed a slightly faster rate than **M4**, and the values of k_{app} increased with the proportion of **M3** in feeding: 0.29, 0.37, and 0.45 h^{-1} for **M3**, and 0.21, 0.28, and 0.37 h^{-1} for **M4**, respectively. The k_{app} value of **M3** during copolymerization was lower than that in homopolymerization (0.53 h^{-1}), whereas the opposite trend was observed for **M4**. Next, we determined the reactivity ratios of **M3** and **M4** using the Fineman−Ross method (Table S1, Figure S14), and r_{M3} and r_{M4} were calculated to be 0.27 and 0.93, respectively.[51] This result indicated that the obtained copolymers possess approximately a randomly distributed sequence. The molar mass of copolymers increased almost linearly with increasing the total monomer conversion (≤80%), and the dispersities of the copolymers remained low (<1.2) throughout the whole process (Figure 5c,f,i), demonstrating again the good controllability of the copolymerization.

To obtain copolymers with high molar mass, we carried out the copolymerization at a higher monomer to initiator ratio (($[\mathbf{M3}]_0 + [\mathbf{M4}]_0$)/$[\mathrm{BnOH}]_0$ = 400/1), and five copolymers (**C1**−**C5**) with different compositions were prepared (Table 3). With increasing the feed ratio of **M4** from 10 to 50%, the time needed to reach a relatively high monomer conversion was greatly prolonged. The M_n values of these copolymers are in the range of 27.6−36.2 kDa, and they all have a relatively narrow dispersity ($Đ$ < 1.2). The molar ratio of the **M3** unit to the **M4** unit in the copolymer was calculated from the ^{1}H NMR spectrum (Figure S15), and the molar content of the **M4** unit was determined to be 0.07, 0.16, 0.25, 0.34, and 0.46 for **C1**−**C5**, respectively, being generally consistent with the monomer feed ratio.

Table 3. Synthesis and Characterization of Copolymers C1−C5[a]

	feed ratio/%[b]			conv./%[c]				
copolymer	M3	M4	time/h	M3	M4	M4%[d]	M_n/kDa[e]	$Đ$[e]
C1	90	10	24	88	82	7	36.2	1.10
C2	80	20	41	82	73	16	34.7	1.14
C3	70	30	70	82	74	25	29.3	1.12
C4	60	40	80	79	70	34	27.6	1.09
C5	50	50	80	91	82	46	29.3	1.14

[a]All copolymerizations were conducted in DCM at 30 °C in a glovebox under N_2 using BnOH as the initiator and DBU/TU as the catalyst. ($[\mathbf{M3}]_0 + [\mathbf{M4}]_0$)/$[\mathrm{BnOH}]_0$/[DBU]/[TU] = 400/1/1/5, $[\mathbf{M3}]_0 + [\mathbf{M4}]_0$ = 0.5 M in DCM. [b]Molar ratio in feed. [c]Determined by ^{1}H NMR spectra. [d]Percentage molar fraction of **M4** in copolymers determined by ^{1}H NMR (Figure S15). [e]Determined by SEC.

The thermal properties of **C1**−**C5** were explored by TGA and DSC (Table 4, Figure S16). All these copolymers are thermally stable with $T_{d,5\%}$ values in the range of 283−292 °C. DSC results revealed that each of the copolymers showed a T_g but did not exhibit any endothermic peak, demonstrating their amorphous structures. The T_g values were increased monotonically from 62.4 °C for **C1** to 87.8 °C for **C5**. These experimental values are close to the theoretical ones calculated from the Fox equation, indicating a relatively random distribution of the two monomer units in the copolymers. The mechanical properties of **C1**−**C5** were also investigated by tensile tests (Table 4 and Figure S17). As expected, the composition of copolymers exerts a significant effect on their mechanical property. With increasing the amount of the **M4** unit, the values of E and σ_y gradually increased while ε_b showed an opposite tendency. Copolymer **C5** showed a brittle character because of its largest fraction of the steric **M4** unit content among the tested copolymers. Overall, the thermal and mechanical properties of these PEA copolymers could be easily manipulated by changing the ratio of two monomer units, affording PEAs from strong brittle plastic to ductile polymeric materials.

Depolymerization of PEAs and Monomer Recovery. We previously reported that the PEAs obtained by the ROP of MDs could be quantitatively and rapidly alcoholyzed into MD precursors at ambient temperature in the presence of a catalytic amount of TBD, but the obtained degradation products need further cyclization procedure to generate MDs. Moreover, the depolymerization of the MD-derived PEAs in toluene under acid catalysis could directly recover the MD monomers, yet this process needs a large amount of solvent.[27] Recycling of a polymer by its bulk thermal depolymerization, with or without the assistance of a matrix, represents another promising method. Monomers could be recovered by distillation or sublimation, avoiding the usage of organic solvents and the plausible complex process of monomer purification.[16,52] Herein, we tested the bulk thermal recycling of PEA polymers using the sublimation method, using $Sn(Oct)_2$ as a catalyst to promote transesterification and PEO as the reaction medium. Upon heating at 140 °C for 4 h in vacuo, polymer **P1b** was depolymerized into its monomer **M1** with high purity (>95%) in a yield of 95−97% (Figure S18 and Table S2, entries 1 and 2). Similarly, **P2b** and **P3b** could also be converted to their corresponding monomers (**M2** and **M3**) with a high purity and yield (>90%) under similar conditions (Figure S19 and Table S2, entries 3−8). Among these PEA homopolymers, polymer **P3b** with the longest pendent *n*-alkyl group needed a longer sublimation time to

Table 4. Thermal and Mechanical Properties of Copolymers C1−C5

copolymer	T_d (°C)[a]	T_g (°C)[b]	$T_{g,fox}$ (°C)[c]	E (MPa)[d]	σ_y (MPa)[d]	σ_b (MPa)[d]	ε_b (%)[d]
C1	292	62.4	62.6	541 ± 7	28.7 ± 0.4	20.9 ± 1.0	382.3 ± 19.4
C2	289	66.0	65.7	668 ± 17	34.6 ± 2.1	17.3 ± 1.8	101.4 ± 10.0
C3	285	70.3	69.3	705 ± 59	39.2 ± 0.5	20.1 ± 0.5	35.5 ± 3.7
C4	283	74.8	73.3	840 ± 40	47.7 ± 1.0	27.5 ± 1.4	18.5 ± 3.5
C5	284	87.8	79.8	966 ± 56	—	46.8 ± 5.6	5.6 ± 0.8

[a]Determined by TGA. [b]Determined by DSC. [c]Calculated according to the Fox equation: $1/T_{g,fox} = \omega_1/T_{g,P3} + \omega_2/T_{g,P4}$, ω_1 and ω_2 represent the weight fraction of **M3** and **M4**, respectively. [d]Determined by uniaxial tensile tests.

https://doi.org/10.1021/acs.macromol.2c00221
Macromolecules 2022, 55, 4000−4010

obtain a high monomer recycling efficiency (Figure 6 and Table S2, entries 6–8). Furthermore, copolymer **C5** was

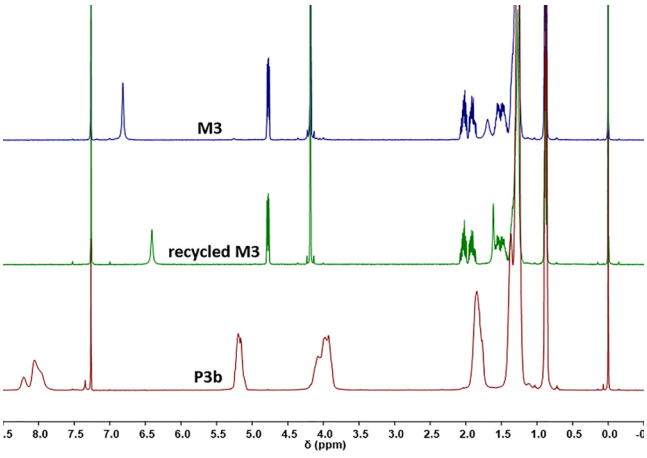

Figure 6. ^{1}H NMR spectra of **P3b**, pristine, and the recycled **M3**.

depolymerized into a mixture of **M3** and **M4** in a total recovering yield of 93% upon heating at 140 °C in vacuo for 8 h (Figure S20 and Table S2, entry 9). Finally, all the recycled monomers could be directly reused for the ROP to afford PEAs because of their high purity (Figure S21).

CONCLUSIONS

We have synthesized four 6-substituted MD monomers (**M1**–**M4**) with *n*-butyl, *n*-hexyl, *n*-octyl, and cyclohexyl groups, respectively, by Passerini-type reaction and the subsequent acid-catalyzed intramolecular cyclization. All of them can undergo controlled ROP to generate PEA homo- or copolymers with high molar masses and narrow dispersities. These PEAs are amorphous and thermally stable with $T_{d,5\%}$ above 260 °C. Their T_gs were influenced greatly by the flexibility of pendent alkyl groups but exhibited only a modest dependence on the *n*-alkyl length because of the hydrogen bonding between the amide groups. However, both the chain length and rigidity of the pendent alkyl groups exerted a significant effect on the mechanical properties of PEAs. By changing the structure of the pendent alkyl groups, we could manipulate the mechanical properties of the PEAs from brittle (**P1** or **C5**) to ductile (**P2**, **P3**, or **C1**), with a wide range of E (1270–541 MPa), σ_b (51–15 MPa), and ε_b (4.0–330%) values. Moreover, the bulk thermal depolymerization of these PEA homo- or copolymers by sublimation could recover monomers with a high efficiency, and the purity of them was high enough for the direct ROP to regenerate the PEA (co)polymers.

ASSOCIATED CONTENT

Supporting Information

The Supporting Information is available free of charge at https://pubs.acs.org/doi/10.1021/acs.macromol.2c00221.

Additional experimental procedures, NMR spectra of monomers, NMR and MALDI-TOF MS spectra of polymers **P1**–**P3**, 2D-WAXD patterns of **P1c** and **P2c**, tensile deformation schematic diagram, ^{1}H NMR spectra and SEC traces of copolymerization kinetics studies, thermal and mechanical properties of copolymers **C1**–**C5**, and ^{1}H NMR spectra of recycled monomers (PDF)

AUTHOR INFORMATION

Corresponding Authors

Fu-Sheng Du – *Beijing National Laboratory for Molecular Sciences, Key Laboratory of Polymer Chemistry and Physics of Ministry of Education, Center for Soft Matter Science and Engineering, College of Chemistry & Molecular Engineering, Peking University, Beijing 100871, China;* orcid.org/0000-0003-3174-6107; Phone: +86-10-62757155; Email: fsdu@pku.edu.cn

Zi-Chen Li – *Beijing National Laboratory for Molecular Sciences, Key Laboratory of Polymer Chemistry and Physics of Ministry of Education, Center for Soft Matter Science and Engineering, College of Chemistry & Molecular Engineering, Peking University, Beijing 100871, China;* orcid.org/0000-0002-0746-9050; Phone: +86-10-62755543; Email: zcli@pku.edu.cn

Authors

Yu-Ting Guo – *Beijing National Laboratory for Molecular Sciences, Key Laboratory of Polymer Chemistry and Physics of Ministry of Education, Center for Soft Matter Science and Engineering, College of Chemistry & Molecular Engineering, Peking University, Beijing 100871, China*

Changxia Shi – *Beijing National Laboratory for Molecular Sciences, Key Laboratory of Polymer Chemistry and Physics of Ministry of Education, Center for Soft Matter Science and Engineering, College of Chemistry & Molecular Engineering, Peking University, Beijing 100871, China*

Tian-Yi Du – *Beijing National Laboratory for Molecular Sciences, Key Laboratory of Polymer Chemistry and Physics of Ministry of Education, Center for Soft Matter Science and Engineering, College of Chemistry & Molecular Engineering, Peking University, Beijing 100871, China*

Xiang-Yue Cheng – *Beijing National Laboratory for Molecular Sciences, Key Laboratory of Polymer Chemistry and Physics of Ministry of Education, Center for Soft Matter Science and Engineering, College of Chemistry & Molecular Engineering, Peking University, Beijing 100871, China*

Complete contact information is available at: https://pubs.acs.org/10.1021/acs.macromol.2c00221

Notes

The authors declare no competing financial interest.

ACKNOWLEDGMENTS

This work was financially supported by the National Natural Science Foundation of China (No. 21871014).

REFERENCES

(1) Rochman, C. M.; Browne, M. A.; Halpern, B. S.; Hentschel, B. T.; Hoh, E.; Karapanagioti, H. K.; Rios-Mendoza, L. M.; Takada, H.; Teh, S.; Thompson, R. C. Classify Plastic Waste as Hazardous. *Nature* **2013**, *494*, 169–171.

(2) Geyer, R.; Jambeck, J. R.; Law, K. L. Production, Use, and Fate of All Plastics Ever Made. *Sci. Adv.* **2017**, *3*, No. e1700782.

(3) Jambeck, J. R.; Geyer, R.; Wilcox, C.; Siegler, T. R.; Perryman, M.; Andrady, A.; Narayan, R.; Law, K. L. Plastic Waste Inputs from Land into the Ocean. *Science* **2015**, *347*, 768–771.

(4) Haider, T. P.; Voelker, C.; Kramm, J.; Landfester, K.; Wurm, F. R. Plastics of the Future? The Impact of Biodegradable Polymers on the Environment and on Society. *Angew. Chem., Int. Ed.* **2019**, *58*, 50–62.

(5) Mecking, S. Nature or Petrochemistry? Biologically Degradable Materials. *Angew. Chem., Int. Ed.* **2004**, *43*, 1078–1085.

(6) Schyns, Z. O. G.; Shaver, M. P. Mechanical Recycling of Packaging Plastics: A Review. *Macromol. Rapid Commun.* **2021**, *42*, No. 2000415.
(7) Rahimi, A.; García, J. M. Chemical Recycling of Waste Plastics for New Materials Production. *Nat. Rev. Chem.* **2017**, *1*, 46.
(8) Hong, M.; Chen, E. Y. X. Chemically Recyclable Polymers: A Circular Economy Approach to Sustainability. *Green Chem.* **2017**, *19*, 3692−3706.
(9) Coates, G. W.; Getzler, Y. D. Y. L. Chemical Recycling to Monomer for an Ideal, Circular Polymer Economy. *Nat. Rev. Mater.* **2020**, *5*, 501−516.
(10) Tang, X.; Chen, E. Y. X. Toward Infinitely Recyclable Plastics Derived from Renewable Cyclic Esters. *Chem* **2019**, *5*, 284−312.
(11) Shi, C.; Reilly, L. T.; Kumar, V. S. P.; Coile, M. W.; Nicholson, S. R.; Broadbelt, L. J.; Beckham, G. T.; Chen, E. Y. X. Design Principles for Intrinsically Circular Polymers with Tunable Properties. *Chem* **2021**, *7*, 2896−2912.
(12) Zhu, J.; Watson, E. M.; Tang, J.; Chen, E. Y. X. A Synthetic Polymer System with Repeatable Chemical Recyclability. *Science* **2018**, *360*, 398−403.
(13) Zhu, J.; Chen, E. Y. X. Living Coordination Polymerization of a Six-Five Bicyclic Lactone to Produce Completely Recyclable Polyester. *Angew. Chem., Int. Ed.* **2018**, *57*, 12558−12562.
(14) MacDonald, J. P.; Shaver, M. P. An Aromatic/Aliphatic Polyester Prepared via Ring-Opening Polymerisation and Its Remarkably Selective and Cyclable Depolymerisation to Monomer. *Polym. Chem.* **2016**, *7*, 553−559.
(15) Shi, C.; Li, Z.-C.; Caporaso, L.; Cavallo, L.; Falivene, L.; Chen, E. Y. X. Hybrid Monomer Design for Unifying Conflicting Polymerizability, Recyclability, and Performance Properties. *Chem* **2021**, *7*, 670−685.
(16) Li, L.-G.; Wang, Q.-Y.; Zheng, Q.-Y.; Du, F.-S.; Li, Z.-C. Tough and Thermally Recyclable Semiaromatic Polyesters by Ring-Opening Polymerization of Benzo-thia-caprolactones. *Macromolecules* **2021**, *54*, 6745−6752.
(17) Fahnhorst, G. W.; Hoye, T. R. A Carbomethoxylated Polyvalerolactone from Malic Acid: Synthesis and Divergent Chemical Recycling. *ACS Macro Lett.* **2018**, *7*, 143−147.
(18) Schneiderman, D. K.; Vanderlaan, M. E.; Mannion, A. M.; Panthani, T. R.; Batiste, D. C.; Wang, J. Z.; Bates, F. S.; Macosko, C. W.; Hillmyer, M. A. Chemically Recyclable Biobased Polyurethanes. *ACS Macro Lett.* **2016**, *5*, 515−518.
(19) Fonseca, A. C.; Gil, M. H.; Simoes, P. N. Biodegradable Poly(ester amide)s-a Remarkable Opportunity for the Biomedical Area: Review on the Synthesis, Characterization and Applications. *Prog. Polym. Sci.* **2014**, *39*, 1291−1311.
(20) Winnacker, M.; Rieger, B. Poly(ester amide)s: Recent Insights into Synthesis, Stability and Biomedical Applications. *Polym. Chem.* **2016**, *7*, 7039−7046.
(21) Keul, H.; Robertz, B.; Hocker, H. New Alternating Poly(amide-ester)s: Synthesis and Properties. *Macromol. Symp.* **1999**, *144*, 47−61.
(22) Liang, Y.; Pan, J.-L.; Sun, L.-H.; Ma, J.-M.; Jiang, H.; Li, Z.-L. Alternating Sequence Control for Poly(ester amide)s by Organocatalyzed Ring-Opening Polymerization. *Macromol. Rapid Commun.* **2019**, *40*, No. 1900435.
(23) Feng, Y.; Lu, J.; Behl, M.; Lendlein, A. Progress in Depsipeptide-Based Biomaterials. *Macromol. Biosci.* **2010**, *10*, 1008−1021.
(24) Feng, Y.; Guo, J. Biodegradable Polydepsipeptides. *Int. J. Mol. Sci.* **2009**, *10*, 589−615.
(25) In't Veld, P. J. A.; Dijkstra, P. J.; Feijen, J. Synthesis of Biodegradable Polyesteramides with Pendant Functional Groups. *Macromol. Chem. Phys.* **1992**, *193*, 2713−2730.
(26) Franz, N.; Klok, H.-A. Synthesis of Functional Polydepsipeptides Via Direct Ring-Opening Polymerization and Post-Polymerization Modification. *Macromol. Chem. Phys.* **2010**, *211*, 809−820.
(27) Shi, C.; Guo, Y.; Wu, Y.; Li, Z.; Wang, Y.; Du, F.; Li, Z. Synthesis and Controlled Organobase-Catalyzed Ring-Opening Polymerization of Morpholine-2,5-Dione Derivatives and Monomer Recovery by Acid-Catalyzed Degradation of the Polymers. *Macromolecules* **2019**, *52*, 4260−4269.
(28) Shi, C.; McGraw, M. L.; Li, Z.-C.; Cavallo, L.; Falivene, L.; Chen, E. Y. X. High-Performance Pan-Tactic Polythioesters with Intrinsic Crystallinity and Chemical Recyclability. *Sci. Adv.* **2020**, *6*, No. eabc0495.
(29) Shi, C.; Clarke, R. W.; McGraw, M. L.; Chen, E. Y. X. Closing the "One Monomer-Two Polymers-One Monomer" Loop Via Orthogonal (De)Polymerization of a Lactone/Olefin Hybrid. *J. Am. Chem. Soc.* **2022**, *144*, 2264−2275.
(30) Boyle, B. M.; Heinz, O.; Miyake, G. M.; Ding, Y. Impact of the Pendant Group on the Chain Conformation and Bulk Properties of Norbornene Imide-Based Polymers. *Macromolecules* **2019**, *52*, 3426−3434.
(31) Baker, G. L.; Vogel, E. B.; Smith, M. R., III Glass Transitions in Polylactides. *Polym. Rev.* **2008**, *48*, 64−84.
(32) Clamor, C.; Cattoz, B. N.; Wright, P. M.; O'Reilly, R. K.; Dove, A. P. Controlling the Crystallinity and Solubility of Functional Pcl with Efficient Post-Polymerisation Modification. *Polym. Chem.* **2021**, *12*, 1983−1990.
(33) Pratt, R. C.; Lohmeijer, B. G. G.; Long, D. A.; Lundberg, P. N. P.; Dove, A. P.; Li, H.; Wade, C. G.; Waymouth, R. M.; Hedrick, J. L. Exploration, Optimization, and Application of Supramolecular Thiourea-Amine Catalysts for the Synthesis of Lactide (Co)Polymers. *Macromolecules* **2006**, *39*, 7863−7871.
(34) Kumar, J. S.; Jonnalagadda, S. C.; Mereddy, V. R. An Efficient Boric Acid-Mediated Preparation of Alpha-Hydroxyamides. *Tetrahedron Lett.* **2010**, *51*, 779−782.
(35) Dirauf, M.; Bandelli, D.; Weber, C.; Goerls, H.; Gottschaldt, M.; Schubert, U. S. TBD-Catalyzed Ring-Opening Polymerization of Alkyl-Substituted Morpholine-2,5-Dione Derivatives. *Macromol. Rapid Commun.* **2018**, *39*, No. 1800433.
(36) Lian, J.; Li, M.; Wang, S.; Tao, Y.; Wang, X. Organocatalytic Polymerization of Morpholine-2,5-Diones toward Methionine-Containing Poly(ester amide)s: Preparation and Facile Functionalization. *Macromolecules* **2020**, *53*, 10830−10836.
(37) Burton, T. F.; Pinaud, J.; Giani, O. Rapid and Controlled Organocatalyzed Ring-Opening Polymerization of 3S-(Isobutyl)-Morpholine-2,5-Dione and Copolymerization with Lactide. *Macromolecules* **2020**, *53*, 6598−6607.
(38) Jing, F.; Smith, M. R., III; Baker, G. L. Cyclohexyl-Substituted Polyglycolides with High Glass Transition Temperatures. *Macromolecules* **2007**, *40*, 9304−9312.
(39) Engelberg, I.; Kohn, J. Physicomechanical Properties of Degradable Polymers Used in Medical Applications: A Comparative Study. *Biomaterials* **1991**, *12*, 292−304.
(40) Worch, J. C.; Prydderch, H.; Jimaja, S.; Bexis, P.; Becker, M. L.; Dove, A. P. Stereochemical Enhancement of Polymer Properties. *Nat. Rev. Chem.* **2019**, *3*, 514−535.
(41) Rogers, S. S.; Mandelkern, L. Glass Formation in Polymers.1. The Glass Transitions of the Poly-(*N*-Alkyl Methacrylates). *J. Phys. Chem.* **1957**, *61*, 985−991.
(42) Kunal, K.; Robertson, C. G.; Pawlus, S.; Hahn, S. F.; Sokolov, A. P. Role of Chemical Structure in Fragility of Polymers: A Qualitative Picture. *Macromolecules* **2008**, *41*, 7232−7238.
(43) Liu, Q.; Wang, C.; Guo, Y.; Peng, C.; Narayanan, A.; Kaur, S.; Xu, Y.; Weiss, R. A.; Joy, A. Opposing Effects of Side-Chain Flexibility and Hydrogen Bonding on the Thermal, Mechanical, and Rheological Properties of Supramolecularly Cross-Linked Polyesters. *Macromolecules* **2018**, *51*, 9294−9305.
(44) Jaffe, M.; Ophir, Z.; Collins, G.; Recber, A.; Yoo, S. U.; Rafalko, J. J. Process-Structure-Property Relationships of Erodable Polymeric Biomaterials: II-Long Range Order in Poly (Desaminotyrosyl Arylates). *Polymer* **2003**, *44*, 6033−6042.
(45) Skrovanek, D. J.; Painter, P. C.; Coleman, M. M. Hydrogen-Bonding in Polymers. 2. Infrared Temperature Studies of Nylon-11. *Macromolecules* **1986**, *19*, 699−705.
(46) Peng, X.; Behl, M.; Zhang, P.; Mazurek-Budzynska, M.; Razzaq, M. Y.; Lendlein, A. Hexyl-Modified Morpholine-2,5-Dione-Based

Oligodepsipeptides with Relatively Low Glass Transition Temperature. *Polymer* **2016**, *105*, 318−326.
(47) Kwok, M.-H.; Seymour, B. T.; Li, R.; Litt, M. H.; Zhao, B.; Zhu, L. Tacticity Effect on Mesogen-Free Liquid Crystalline Self-Assembly Induced by Strong Dipole-Dipole Interactions. *Macromolecules* **2019**, *52*, 3601−3611.
(48) Beiner, M.; Huth, H. Nanophase Separation and Hindered Glass Transition in Side-Chain Polymers. *Nat. Mater.* **2003**, *2*, 595−599.
(49) Gao, C.; Yu, L.; Liu, H.; Chen, L. Development of Self-Reinforced Polymer Composites. *Prog. Polym. Sci.* **2012**, *37*, 767−780.
(50) Hong, M.; Tang, X.; Newell, B. S.; Chen, E. Y. X. "Nonstrained" Gamma-Butyrolactone-Based Copolyesters: Copolymerization Characteristics and Composition-Dependent (Thermal, Eutectic, Cocrystallization, and Degradation) Properties. *Macromolecules* **2017**, *50*, 8469−8479.
(51) Fineman, M.; Ross, S. D. Linear Method for Determining Monomer Reactivity Ratios in Copolymerization. *J. Polym. Sci.* **1950**, *5*, 259−262.
(52) Loyd, E. M.; Hernandez, H. L.; Feinberg, A. M.; Yourdkhani, M.; Zen, E. K.; Mejia, E. B.; Sottos, N. R.; Moore, J. S.; White, S. R. Fully Recyclable Metastable Polymers and Composites. *Chem. Mater.* **2019**, *31*, 398−406.

https://doi.org/10.1021/acs.macromol.2c00221
Macromolecules 2022, 55, 4000−4010